Microporous Materials

DOI: 10.1002/ange.201101909

The Synthesis of Chiral Periodic Organosilica Materials with Ultrasmall Mesopores**

*Xiaowei Wu, Thomas Blackburn, Jonathan D. Webb, Alfonso E. Garcia-Bennett, and Cathleen M. Crudden**

The assembly of small molecule precursors into helical architectures is a common motif in nature, and is often a critical component of the function of the resulting supramolecular assemblies, such as in DNA.[1,2] Inspired by these architectures, materials chemists have prepared similar morphologies in the lab, for example by the application of templated sol–gel methods.[3] Interestingly, helical materials can be prepared in the absence of other chiral directors, for example using achiral surfactants,[4–10] but these techniques lead to equal amounts of both helical forms. For non-racemic helical structures, specially designed chiral, enantiomerically enriched surfactants are required.[11–13] Despite the advantages of organosilica materials in contrast to entirely inorganic materials,[14] there are few reports of purely organic chiral PMOs (Periodic Mesoporous Organosilica) made by the incorporation of chiral monomers into the walls,[15,16] and even fewer reports of helical morphology in porous organosilicas.[17,18] Furthermore, the powerful strategy of the use of chiral co-monomers to control morphology and helicity has received remarkably little attention. As we will demonstrate, organosilica materials offer novel methods for introduction of chirality that do not require the use of specialized surfactants, and result in direct incorporation of the chiral units into the backbone of the material, thus offering greater possibilities for control over material properties than grafting methods.

Since our previous work on chirality transfer in organosilica materials relies on π–π stacking,[16] and since such interactions have been shown to be important in other helical materials,[3] we began our studies by employing the phenylene-bridged monomer $(EtO)_3Si\text{-}C_6H_4\text{-}Si(OEt)_3$ as the structural unit. To date, there has been only one report of this monomer generating helical materials, which required the use of a specialized template.[15]

Herein we report a simple method to synthesize ordered chiral helical organosilicas with ultrasmall mesopores using, for the first time, a chiral dopant in the form of a co-monomer in such helical structures.[16] This strategy enables us to exert control of the structure by the type and nature of the co-monomer employed. Importantly, it also permits the introduction of functionality into the material, for example in the form of alkoxy groups that can serve as a handle for further chemical manipulation.[19,20] Remarkably, the synthesis of these hybrid materials can be affected in under 1 hour. It is also interesting to note that all of the porous inorganic and hybrid helical materials reported to date have relatively large pores,[4–10,18] despite the fact that it is at smaller length scales that chiral interactions between the material and molecular species are likely to be strongest. Thus the potential for chiral helical hybrid organic silica materials (HHOM) with pores in the range described herein is significant.[21]

The chiral co-monomer **4** was prepared as shown in Scheme 1. Binaphthol was chosen as the backbone for the chiral co-monomer as it is known to be a privileged structure

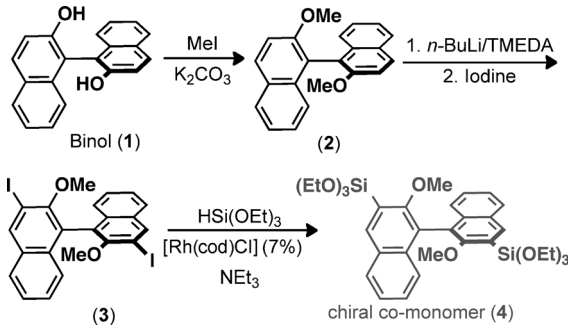

Scheme 1. Synthesis of chiral co-monomer **4**. TMEDA = *N*,*N*,*N*′,*N*′-tetramethylethylenediamine, cod = 1,5-cyclooctadiene.

in catalysis,[22] and has strong ability to transfer chiral information in soft materials, such as liquid crystals,[23a] and in hard materials, such as self-assembled porphyrin–silica hybrids.[23b] Additionally, binol is readily available in both enantiomeric forms. To incorporate binol directly into the backbone of the material, we employed the route shown in Scheme 1. After methylation of the free hydroxy groups, directed *ortho* metalation followed by trapping with I_2 is used to introduce iodine atoms adjacent to the methoxy groups.[24a,b] A final rhodium-catalyzed Masuda coupling[24c] results in a facile three-step route to **4**. Critically, the attachment of the siloxanes directly to the aromatic core results in a rigid

[*] Dr. X. Wu, T. Blackburn, J. D. Webb, Prof. C. M. Crudden
Queen's University, Department of Chemistry
90 Bader Lane, Kingston, ON (Canada)
E-mail: cruddenc@chem.queensu.ca
Homepage: http://www.cruddengroup.com
Dr. A. E. Garcia-Bennett
Nanotechnology and Functional Materials
Department of Engineering Sciences, The Ångström Laboratory
Uppsala University, 75121 Uppsala (Sweden)

[**] The Natural Sciences and Engineering Research Council of Canada, the Canada Foundation for Innovation, Queen's University, and Silicycle Inc. are acknowledged for support of this research. A.E.G.-B. is grateful to the Swedish Research Council, Vetenskapsrådet for funding.

Supporting information for this article is available on the WWW under http://dx.doi.org/10.1002/anie.201101909.

chiral unit that is unique from other approaches that incorporate binol into materials with flexible alkyl tethers.[20]

With a scalable synthesis of **4** in hand, the synthesis of HHOMs was affected by employing 1,4-bis(triethoxylsilyl)-benzene BTEB (**5**) as the bulk organosilica monomer, with varying amounts of **4** under basic conditions with cetyltrimethylammonium bromide CTAB as the surfactant. The reaction was complete in under one hour (Scheme 2). Materials were prepared with 0, 7, 14, and 21 mol% of **4** in BTEB (**5**): HHOM-0, HHOM-7, HHOM-14, and HHOM-21, respectively. SEM and TEM images of the resulting materials are shown in Figure 1.

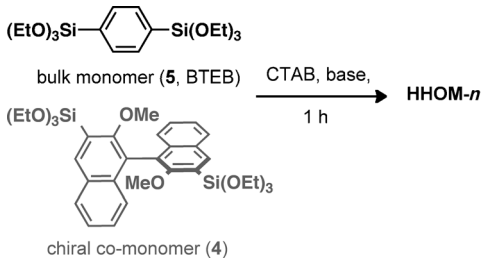

Scheme 2. Synthesis of helical hybrid organic silica materials (HHOMs).

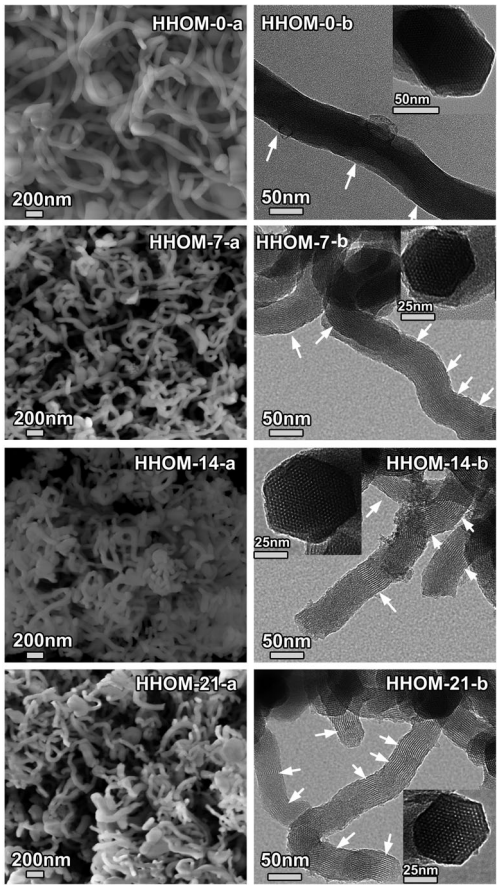

Figure 1. SEM and TEM images showing the morphology and mesostructure of the extracted samples synthesized with different molar ratios of **4**/**5**: HHOM-0 (mol% **4** = 0), HHOM-7 (mol% **4** = 7), HHOM-14 (mol% **4** = 14), and HHOM-21 (mol% **4** = 21). The arrows indicate the fringes on the images.

SEM and TEM images showed that HHOM–0, prepared without chiral co-monomer **4**, has a helical fiber-like morphology with a fiber length of 1–2 μm, diameter of 70 nm, and pitch length of 0.5 μm–1.5 μm. Materials prepared with co-monomer **4** were more twisted and had smaller particle diameters than materials prepared without this chiral species (Supporting Information, Figure S1. Importantly, this effect increases as the amount of **4** increases. The outer diameters, carefully determined from HRTEM images, decreased from 70 nm (HHOM) to 50 nm, 47 nm, and 42 nm with increasing quantities of **4**.

It is difficult to accurately measure the length of the particles for HHOMs 7 to 21 owing to their twisted morphology, but they are estimated to be between 0.5 and 2 μm. The pitch length varied from 350 nm to 900 nm for all samples. The TEM images (Figure 1) obtained with the incident beam perpendicular to the rods showed ordered fringes as indicated by the arrows. The HRTEM images of the ends of these materials (insets in Figure 1) show the twisted hexagonal morphology, which is not as clear in the SEM images owing to the small size of the particles. Thus, similar to the pioneering materials reported previously by the Che group,[6,11] these samples can be considered to be chiral periodic organosilica materials with highly ordered 2D hexagonal channels winding around the central axis of solid helical rods, although the extent of twisting (chiral pitch) and the homogeneity of the particles is not as pronounced as observed in the Che-type materials.

The physisorption isotherms are transitional between types I and IV (Figure 2), which is consistent with materials with pore sizes being between micro- and mesoporous.[25] As in isotherms of other supermicroporous and small mesoporous materials, the capillary condensation step occurs in the pressure region typically employed by the BET method (0.05–0.3 P/P_0). Thus, the BET plots were prepared using data on the low side of this region (< 0.15 P/P_0) and the surface area is also calculated from the α_s plot[26,27] (total surface area, S_t) in the linear region (Supporting Information, Figures S2–5).

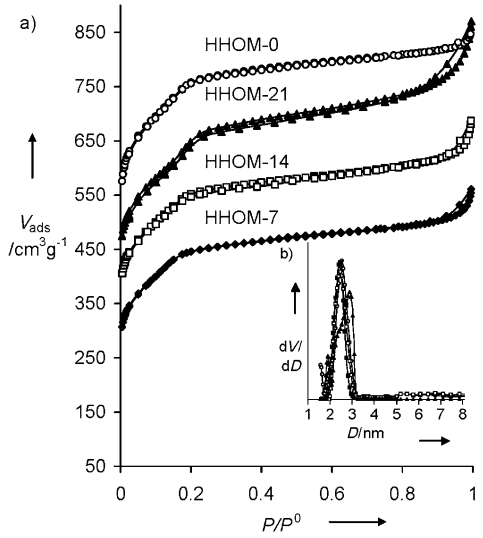

Figure 2. a) N_2 isotherms of the extracted samples in Figure 1. b) The corresponding DFT pore size distribution plots.

Table 1: Physicochemical properties of different HHOMs obtained from N_2 adsorption–desorption isotherms.[a]

Sample	S_{BET} [$m^2 g^{-1}$]	S_t [$m^2 g^{-1}$]	S_e [$m^2 g^{-1}$]	S_p [$m^2 g^{-1}$]	V_p [$cm^3 g^{-1}$]	V_t [$cm^3 g^{-1}$]	D_{DFT} [nm]
HHOM-0	1268	1144	55	1089	0.55	0.70	2.45
HHOM-7	921	879	88	791	0.38	0.56	2.45
HHOM-14	910	897	105	791	0.38	0.60	2.45
HHOM-21	978	931	113	818	0.38	0.81	2.88

[a] S_{BET} is the surface area calculated using the BET method. The small fraction of micropores in HHOM-0 most likely contributes to the discrepancy between S_{BET} and S_t. The total surface area (S_t), external surface area (S_e), primary pore surface area (S_p), and primary pore volume (V_p) were obtained using the α_s-plot method (see Supporting Information, Table S1).[27] V_t is the total pore volume calculated from the amount adsorbed at a relative pressure (P/P_0) of about 0.99. S_e was defined as the sum of the surface area of secondary pores and macropores. Li-Chrospher Si-1000 silica gel ($S_{BET} = 25\ m^2 g^{-1}$) was used as the reference adsorbent in the α_s-plot analysis. D_{DFT} was obtained from density functional calculations.

Both S_{BET} and S_t values are listed in Table 1 for comparative purposes. As expected, the S_{BET} values for all the materials were slightly larger than the corresponding S_t value, which was either due to the presence of a small number of micropores or the differences in interaction with the surface of our materials and the reference material in the α_s method (Table 1). The surface areas and pore volumes (Table 1) of these materials were high, indicating that they are well-ordered and accessible.

Density functional theory (DFT) was employed to evaluate pore size distributions (Figure 2b).[27a] The primary pore sizes are listed in Table 1. For materials with small pores, the BJH model is known to underestimate pore sizes through an overestimation of the transition pressures caused by the effect of the capillary forces on the amount of nitrogen adsorbed.[27a] Conversely, Kruk et al. suggest that NLDFT can underestimate the condensation pressure in pores of given sizes, resulting in an overestimation of the pore size on the basis of experimental adsorption data.[27b] According to DFT analysis, pore sizes are typically around 2.5 nm.

Although the helical morphology can be obtained under a wide range of surfactant concentrations from 0.1 wt% to 1 wt%, it is strongly dependent on the ratio of surfactant to ammonia. As the concentration of ammonia decreases from 28 wt% to 5 wt%, the helical fibers become shorter until at 5 wt%, 500 nm diameter spheres with ultrasmall mesopores (2.5 nm) were obtained (Supporting Information, Figure S7 and Table S2).

The XRD patterns can be indexed by 10, 11, and 20 reflections on the basis of the hexagonal system (Supporting Information, Figure S8), with d(10) spacings of 3.59 nm, 3.53 nm, 3.40 nm, and 3.40 nm for HHOM-0, HHOM-7, HHOM-14, and HHOM-21, respectively. The XRD pattern of HHOM–0 at medium diffraction angles from 6–28° showed two resolved peaks at *d* spacings of 0.85 and 0.43 nm, which provides evidence of some degree of periodic structure within the walls.[28–30] However these peaks were absent for materials containing the chiral co-monomer, suggesting that the inclusion of the chiral co-monomer leads to a disruption in intrawall packing, providing evidence for the successful incorporation of **4** into the materials.

Further confirmation of the incorporation of **4** into the final material comes from the ^{13}C CP-MAS NMR spectra. These spectra exhibit signals from $\delta = 129$ to 137 ppm along with small peaks from ethoxy groups at $\delta = 19$ ppm and $\delta = 62$ ppm (Figure 3). The peak centered at $\delta = 137$ ppm is attributable to the four magnetically equivalent carbon atoms of the 1,4-disubstituted phenyl ring in **5**.[28–30] The peak at about 130 ppm is a composite of three of the strongest signals in the binaphthyl monomer **4** (C5, C7, and C8; see the Supporting Information, Figure S9). When the amount of **4** reaches 21 mol%, a small peak at $\delta = 162$ ppm becomes apparent and was assigned to C2. The relative intensity of these two peaks assigned to **4** increases as the molar ratio of **4** increases, which is consistent with improved incorporation at higher loadings. The absence of Q^n sites in the range of $\delta = -90$ to -125 ppm of the ^{29}Si SP-MAS NMR spectra (Supporting Information, Figure S10) confirmed that any Si–C bond cleavage is so small as to be undetected. At higher loadings of **4** (40 mol% **4**), cleavage of the Si–C bond was observed, and at even higher loadings (60 mol%), a disordered pore structure was observed.

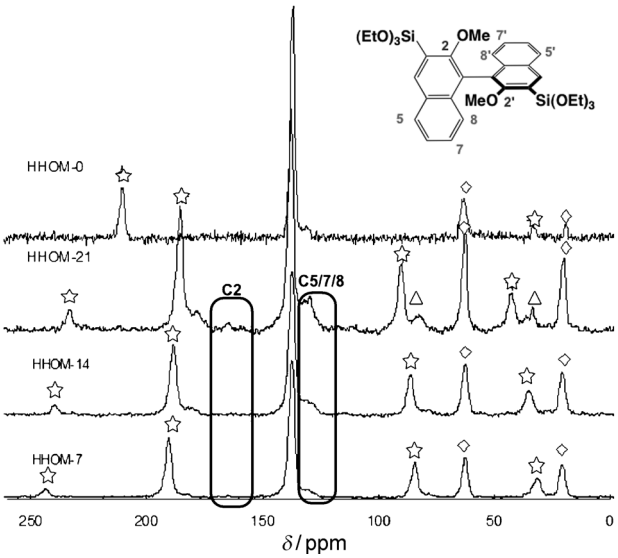

Figure 3. ^{13}C CP-MAS spectra of extracted samples from Figure 1. Stars mark the spinning side bands, and peaks due to residual ethoxy peaks are shown with diamonds. Triangles mark the residual surfactant in HHOM-21.

Thermal analysis of surfactant-free HHMOs was carried out to investigate the composition and thermal stability of the materials under air. Analysis of HHOMs by TGA and DTA (Supporting Information, Figures S11–S14) reveals a decrease in weight between 400–500 °C of 8.5%, 12.1%, and 16.3% for HHOM-7, HHOM-14, and HHOM-21. HHOM-0 shows no loss of mass in this area, which is consistent with this signal being due to loss of chiral co-monomer **4**. The percentage

weight losses observed for the various materials suggest that the incorporation of chiral monomer **4** is closely matched to the initially added amounts of co-monomer **4**.

CD signals obtained from ethanol suspensions of the chiral solid materials closely reproduced those of monomeric *R*-**4** (Supporting Information, Figure S15), with the exception of a slight red shift of 8 nm. When the enantiomer S-**4** was used as the co-monomer, as expected, a mirror image CD was observed.

To quantify the effect of dopant **4** on the helicity of the materials, we attempted to count the number of particles with right- or left-handed helices from randomly chosen helical particles in the SEM images. However, the small particle size and the low curvature of the materials made this estimation difficult to carry out with precision. It is, however, clear from Figure 1 that increases in the amount of co-monomer lead to increasing curvature in the bulk samples, indicating the importance of the inclusion of this co-monomer relative to the material prepared solely from benzene-bridged monomer **5**.

In conclusion, chiral helical organosilica materials with ultrasmall mesopores have been prepared in less than one hour by the incorporation of a chiral co-monomer capable of interacting with the bulk monomer by π stacking. Increasing the amounts of this co-monomer led to increasing curvature of the resulting PMO materials. This effect has previously only been observed with chiral templating agents. The synthesis of novel materials from other chiral co-monomers is currently underway in our laboratories, and results will be reported in due course.

Experimental Section

The synthesis of HHOMs was carried out in a 50 mL glass beaker with an aqueous solution containing the ionic surfactant. Typically, CTAB (0.06 g) was dissolved in concentrated ammonia solution (30 g, 28–30 wt%) at 40°C. BTEB (0.12 g) was then added to the ammonia solution under vigorous stirring for 10 min at 40°C. The mixture was left at 40°C for 1 hour. With regard to the doped HHOMs, *X* g of enantiomerically pure or racemic **4** was added to the solution as the co-precursor. *X* was varied at molar ratios of **4** with respect to **5** (BTEB) of 0%, 7%, 14%, and 21%. In all cases, the as-synthesized powders were extracted with acidic ethanol (36 mL HCl (1M) in 800 mL ethanol) at 70°C for 18 h. The methoxy group is preserved during the extraction procedure (Supporting Information, Figures 16, S17). For full characterization details, see the Supporting Information.

Received: March 17, 2011
Revised: May 7, 2011
Published online: July 13, 2011

Keywords: chirality · helical structures · microporous materials · organosilica · silicon

[1] J. H. Fuhrhop, W. Helfrich, *Chem. Rev.* **1993**, *93*, 1565.
[2] a) L. J. Prins, J. Huskens, F. de Jong, P. Timmerman, D. N. Reinhoudt, *Nature* **1999**, *398*, 498; b) J. C. Nelson, J. G. Saven, J. S. Moore, P. G. Wolynes, *Science* **1997**, *277*, 1793.
[3] a) R. Atluri, N. Hedin, A. E. Garcia-Bennett, *J. Am. Chem. Soc.* **2009**, *131*, 3189; b) J. Hwa Jung, Y. Ono, S. Shinkai, *Angew. Chem.* **2000**, *112*, 1931; *Angew. Chem. Int. Ed.* **2000**, *39*, 1862; c) J. J. E. Moreau, L. Vellutini, M. Wong Chi Man, C. Bied, *J. Am. Chem. Soc.* **2001**, *123*, 1509.
[4] T. Delclos, C. Aime, E. Pouget, A. Brizard, I. Huc, M. H. Delville, R. Oda, *Nano Lett.* **2008**, *8*, 1929.
[5] B. Wang, C. Chi, W. Shan, Y. H. Zhang, N. Ren, W. L. Yang, Y. Tang, *Angew. Chem.* **2006**, *118*, 2142; *Angew. Chem. Int. Ed.* **2006**, *45*, 2088.
[6] X. W. Wu, H. Y. Jin, Z. Liu, T. Ohsuna, O. Terasaki, K. Sakamoto, S. N. Che, *Chem. Mater.* **2006**, *18*, 241.
[7] S. Yang, L. Z. Zhao, C. Z. Yu, X. F. Zhou, J. W. Tang, P. Yuan, D. Y. Chen, D. Y. Zhao, *J. Am. Chem. Soc.* **2006**, *128*, 10460.
[8] L. P. Zhou, G. S. Hong, L. M. Qi, Y. F. Lu, *Langmuir* **2009**, *25*, 6040.
[9] F. Rambaud, K. Valle, S. Thibaud, B. Julian-Lopez, C. Sanchez, *Adv. Funct. Mater.* **2009**, *19*, 2896.
[10] L. Zhang, S. Z. Qiao, Y. G. Jin, L. N. Cheng, Z. F. Yan, G. Q. Lu, *Adv. Funct. Mater.* **2008**, *18*, 3834.
[11] a) S. Che, Z. Liu, T. Ohsuna, K. Sakamoto, O. Terasaki, T. Tatsumi, *Nature* **2004**, *429*, 281; b) S. Che, A. E. Garcia-Bennett, T. Yokoi, K. Sakamoto, H. Kunieda, O. Terasaki, T. Tatsumi, *Nat. Mater.* **2003**, *2*, 801.
[12] Y. G. Yang, M. Suzuki, S. Owa, H. Shirai, K. Hanabusa, *J. Mater. Chem.* **2006**, *16*, 1644.
[13] X. F. Pei, J. Zhang, S. B. Wang, Y. X. Chen, X. J. Wu, Y. Li, B. Z. Li, Y. G. Yang, *J. Sol-Gel Sci. Technol.* **2009**, *50*, 397.
[14] a) F. Hoffmann, M. Fröba, *Chem. Soc. Rev.* **2011**, *40*, 608; b) N. Mizoshita, T. Tani, S. Inagaki, *Chem. Soc. Rev.* **2011**, *40*, 789, and references therein; c) A. Thomas, *Angew. Chem.* **2010**, *122*, 8506; *Angew. Chem. Int. Ed.* **2010**, *49*, 8328, and references therein; d) F. Hoffmann, M. Cornelius, J. Morell, M. Froba, *Angew. Chem.* **2006**, *118*, 3290; *Angew. Chem. Int. Ed.* **2006**, *45*, 3216.
[15] a) A. Kuschel, S. Polarz, *J. Am. Chem. Soc.* **2010**, *132*, 6558; b) M. J. Morell, S. Catterjee, P. J. Klar, D. Mauder, I. Shenderovich, F. Hoffmann, M. Fröba, *Chem. Eur. J.* **2008**, *14*, 5935; c) A. Kuschel, H. Sievers, S. Polarz, *Angew. Chem.* **2008**, *120*, 9655; *Angew. Chem. Int. Ed.* **2008**, *47*, 9513; d) S. Inagaki, S. Guan, Q. Yang, M. P. Kapoor, T. Shimada, *Chem. Commun.* **2008**, 202; e) S. Polarz, A. Kuschel, *Adv. Mater.* **2006**, *18*, 1206; f) A. Die, R. Voss, G. Scholz, G. A. Ozin, M. Antonietti, A. Thomas, *Chem. Mater.* **2007**, *19*, 2649.
[16] S. MacQuarrie, M. P. Thompson, A. Blanc, N. J. Mosey, R. P. Lemieux, C. M. Crudden, *J. Am. Chem. Soc.* **2008**, *130*, 14099.
[17] a) X. J. Meng, T. Yokoi, D. L. Lu, T. Tatsumi, *Angew. Chem.* **2007**, *119*, 7942; *Angew. Chem. Int. Ed.* **2007**, *46*, 7796; b) P. Yuan, L. Z. Zhao, N. A. Liu, G. F. Wei, Y. Zhang, Y. H. Wang, C. Z. Yu, *Chem. Eur. J.* **2009**, *15*, 11319; c) L. F. Bi, Y. Li, S. B. Wang, Z. Y. Zhu, Y. X. Chen, Y. L. Chen, B. Z. Li, Y. G. Yang, *J. Sol-Gel Sci. Technol.* **2010**, *53*, 619.
[18] a) Y. Li, L. F. Bi, S. B. Wang, Y. L. Chen, B. Z. Li, X. L. Zhu, Y. G. Yang, *Chem. Commun.* **2010**, *46*, 2680; b) Y. Li, H. R. Wang, L. W. Wang, F. Zhou, Y. L. Chen, B. B. Li, Y. G. Yang, *Nantoech.* **2011**, *22*, 135605.
[19] Typically, OMe groups are removed by treatment with BBr_3: J. F. W. McOmie, M. L. Watts, D. E. West, *Tetrahedron* **1968**, *24*, 2289.
[20] a) L. Zhang, Y. Guo, J. Peng, X. Liu, P. Yuan, Q. Yang, C. Li, *Chem. Commun.* **2011**, *47*, 4087; b) X. Liu, P. Y. Wang, L. Zhang, J. Yang, C. Li, Q. H. Yang, *Chem. Eur. J.* **2010**, *16*, 12727; c) G. H. Liu, Y. Gao, X. Q. Lu, F. Zhang, M. M. Liu, H. X. Li, *Chem. Commun.* **2008**, 3184; d) K. Pathak, A. P. Bhatt, S. H. R. Abdi, R. I. Kureshy, N. H. Khan, I. Ahmad, R. V. Jasra, *Tetrahedron: Asymmetry* **2006**, *17*, 1506; e) X. Wang, P. Han, X. Qiu, X. Ji, L. Gao, *Catal. Lett.* **2008**, *124*, 418; f) P. Wang, J. Yang, J. Liu, L. Zhang, Q. Yang, *Microporous Mesoporous Mater.* **2009**, *117*, 91.
[21] a) D. Bradshaw, T. J. Prior, E. J. Cussen, J. B. Claridge, M. J. Rosseinsky, *J. Am. Chem. Soc.* **2004**, *126*, 6106; b) A. E. Rowan, R. J. M. Nolte, *Angew. Chem.* **1998**, *110*, 65; *Angew. Chem. Int.*

Ed. **1998**, *37*, 63; c) T. E. Gier, X. H. Bu, P. Y. Feng, G. D. Stucky, *Nature* **1998**, *395*, 154.
[22] a) Y. Chen, S. Yekta, A. K. Yudin, *Chem. Rev.* **2003**, *103*, 3155; b) J. M. Brunel, *Chem. Rev.* **2005**, *105*, 857.
[23] a) G. Gottarelli, M. Hibert, B. Samori, G. Solladie, G. P. Spada, R. Zimmermann, *J. Am. Chem. Soc.* **1983**, *105*, 7318; b) H. Qiu, J. Xie, S. Che, *Chem. Commun.* **2011**, *47*, 2607.
[24] a) S. J. Dolman, K. C. Hultzsch, F. Pezet, X. Teng, A. H. Hoveyda, R. R. Schrock, *J. Am. Chem. Soc.* **2004**, *126*, 10945; b) V. Snieckus, *Chem. Rev.* **1990**, *90*, 879; c) M. Murata, M. Ishikura, M. Nagata, S. Watanabe, Y. Masuda, *Org. Lett.* **2002**, *4*, 1843.
[25] A. Sayari, P. Liu, M. Kruk, M. Jaroniec, *Chem. Mater.* **1997**, *9*, 2499.
[26] M. Jaroniec, M. Kruk, J. P. Olivier, *Langmuir* **1999**, *15*, 5410.
[27] a) P. I. Ravikovitch, S. C. O. Domhnaill, A. V. Neimark, F. Schüth, K. K. Unger, *Langmuir* **1995**, *11*, 4765; b) M. Kruk, M. Jaroniec, A. Sayari, *J. Phys. Chem. B* **1997**, *101*, 583.
[28] S. Inagaki, S. Guan, Y. Fukushima, T. Ohsuna, O. Terasaki, *J. Am. Chem. Soc.* **1999**, *121*, 9611.
[29] Q. H. Yang, M. P. Kapoor, S. Inagaki, *J. Am. Chem. Soc.* **2002**, *124*, 9694.
[30] Y. Yang, A. Sayari, *Chem. Mater.* **2008**, *20*, 2980.

